Available online at www.sciencedirect.com
ScienceDirect
Applied Geochemistry 22 (2007) 534–556
Applied Geochemistry
www.elsevier.com/locate/apgeochem

Halogen concentrations in pore waters and sediments of the Nankai Trough, Japan: Implications for the origin of gas hydrates

Y. Muramatsu [a,*], T. Doi [a], H. Tomaru [b], U. Fehn [b], R. Takeuchi [c], R. Matsumoto [c]

[a] Department of Chemistry, Gakushuin University, Tokyo 171-8588, Japan
[b] Department of Earth & Environmental Sciences, University of Rochester, Rochester, NY 14627, USA
[c] Department of Earth and Planetary Science, University of Tokyo, Tokyo 113-0033, Japan

Available online 28 December 2006

Abstract

Presented here are halogen concentrations (Cl, Br and I) in pore waters and sediments from three deep cores in gas hydrate fields of the Nankai Trough area. The three cores were drilled between 1999 and 2004 in different geologic regions of the northeastern Nankai Trough hydrate zone. Iodine concentrations in all three cores increase rapidly with depth from seawater concentrations (0.00043 mmol/L) to values of up to 0.45 mmol/L. The chemical form of I was identified as I^-, in accordance with the anaerobic conditions in marine sediments below the SO_4 reduction depth. The increase in I is accompanied by a parallel, although lesser increase in Br concentrations, while Cl concentrations are close to seawater values throughout most of the profiles. Large concentration fluctuations of the three halogens in pore waters were found close to the lower boundary of the hydrate stability zone, related to processes of formation and dissociation of hydrates in this zone. Generally low concentrations of I and Br in sediments and the lack of correlation between sediment and pore water profiles speak against derivation of I and Br from local sediments and suggest transport of halogen rich fluids into the gas hydrate fields. Differences in the concentration profiles between the three cores indicate that modes of transportation shifted from an essentially vertical pattern in a sedimentary basin location to more horizontal patterns in accretionary ridge settings. Because of the close association between organic material and I and the similarity of transport behavior for I^- and CH_4, the results suggest that the CH_4 in the gas hydrates also was transported by aqueous fluids from older sediments into the present layers.

1. Introduction

Forearc areas have been recognized as the location of major processes leading to the dewatering of the subducting slab and the overriding wedge, accompanied by the storage or release of major quantities of CH_4. Expression of these processes is the ubiquitous presence of gas hydrates associated with active margins as well as the frequent occurrence of mud volcanoes in forearc locations. Gas hydrates are crystalline structures of water ice which have trapped gas molecules, mostly CH_4 with minor

* Corresponding author.
E-mail address: yasuyuki.muramatsu@gakushuin.ac.jp (Y. Muramatsu).

0883-2927/$ - see front matter © 2007 Elsevier Ltd. All rights reserved.
doi:10.1016/j.apgeochem.2006.12.015

additions of higher hydrocarbons (Sloan, 1998). They are common along all continental margins in water depths typically greater than 800 m within 50–400 m below the seafloor. The lower boundary of the stability field for gas hydrates depends on the thermal gradient in a given location and is indicated by a strong seismic reflector, called the bottom simulating reflector (BSR). Below the BSR, gas hydrates are not stable, but the area typically contains considerable amounts of free gas. The frequent recognition of BSRs in seismic surveys has led to estimates that the amount of C present in gas hydrates is of similar magnitude as all of the traditional fossil fuel reservoirs combined (e.g. Kvenvolden, 1999), although the precise quantity is still debated (e.g. Milkov et al., 2003). Because gas hydrates have been recognized as an important C reservoir, they have been mentioned prominently as a potentially large source of energy and of greenhouse gases (Kvenvolden, 1999), but are increasingly also invoked in discussions concerning the global C cycle and rapid changes in ocean circulation and climate (e.g. Dickens et al., 1997; Dickens, 2001; Kastner, 2001; Kennett et al., 2003). Although the occurrence of gas hydrates is not restricted to active continental margins, the presence and formation of gas hydrates in active margins has attracted increased attention, specifically during recent ODP Legs (201 and 204), IODP expedition 311 and in several large projects on gas hydrates in the Nankai area, carried out by Japanese organizations. The origin of the fluids and, more specifically, of the CH_4 in the fluids in these settings is still a major topic of debate. The three halogen elements used for the investigation presented here can give important clues on the origin and formation of gas hydrate occurrences, mainly related to the different degrees of association with organic material shown by these elements: they range from the strongly biophilic characteristic of I to the essentially conservative behavior of Cl in waters associated with gas hydrates, with Br taking a position in between the other two elements. It is possible that Br is also derived from silicate weathering (Martin, 1999). While Cl concentrations are determined routinely in cores from the ODP program or similar activities, I and Br concentrations are less commonly measured. The strong enrichment of I in pore waters associated with gas hydrate fluids was shown first at the Peru Margin (Martin et al., 1993), and has been found in the meantime in all marine gas hydrate locations where I has been determined (e.g. Egeberg and Dickens, 1999; Fehn et al., 2003; Fehn et al., 2006). Because of the close association of I with organic matter and the similarity in diffusion coefficients between I^- and CH_4, it is likely that these two compounds are transported together in aqueous fluids and that I can be used as a proxy for the origin of CH_4 in gas hydrate fields.

Results are reported here from three deep cores taken from gas hydrate fields in the Nankai Trough area. The cores were taken within a program organized by the Japanese Ministry of Economy, Trade and Industry (METI) between 1999 and 2004. The three cores reached depths between 243 and 342 mbsf, and went in all cases below the BSR, i.e. covering the entire thickness of the gas hydrate occurrence and parts of the underlying sections containing free gas. Results are reported here of determinations of Cl, Br and I concentrations in pore waters and associated sediment samples taken from these cores. Overall, the three halogens were determined in 281 pore water samples; I and Br were measured in 111 sediment samples.

2. Geologic setting

The Nankai Trough formed by the subduction of the Philippine Sea Plate under the Eurasian Plate and is associated with an accretionary margin running roughly parallel to the eastern coast of southern Honshu, Shikoku and Kyushu (Fig. 1a). It has been the focus of several drilling expeditions: ODP drilling was focused on the accretionary wedge in the mid section of the trough area (e.g. ODP Legs 808; 1178), and recent investigations organized by Japanese research groups took place in the northeastern section of the Nankai Trough area. Samples recovered from drill sites in the gas hydrate area are the focus of this investigation (Fig. 1b).

A schematic cross section through the Nankai margin is shown in Fig. 2, which also indicates the different tectonic settings of the gas hydrate fields in this area (Baba and Yamada, 2004). The subducted crust in the Nankai Trough is about 20 Ma (Jarrard, 1986) with a relatively thin package of subducting marine sediments (<2 km; Hyndman et al., 1992). The accretionary prism is bounded by a ridge, separating it from the sedimentary basin formed between the currently active accretionary wedge and the remnants of an earlier subduction configuration. This prism was generated when the Pacific Plate was subducted under the Eurasian Plate in this region and the proto-Izu Bonin Arc

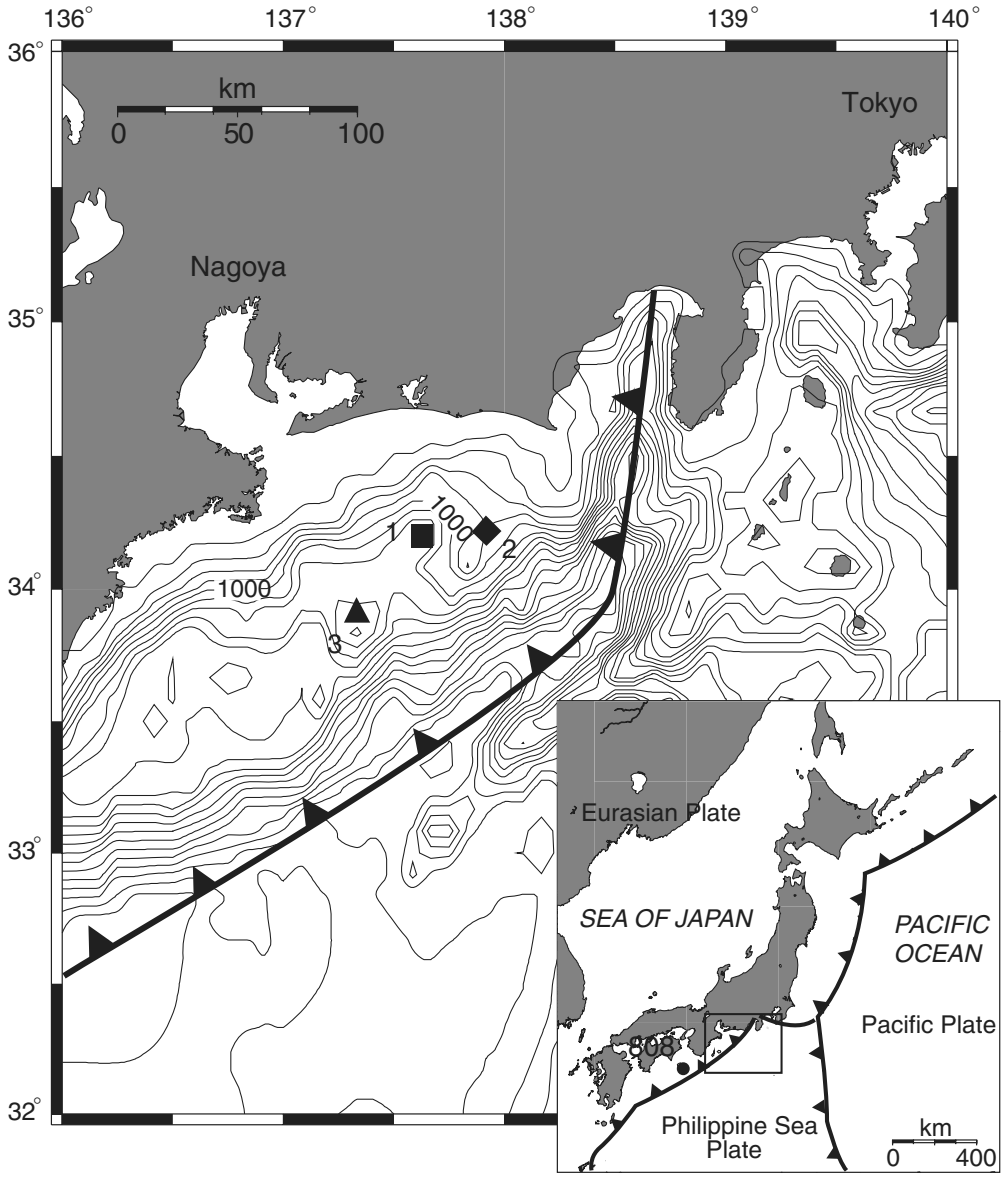

Fig. 1. General tectonic setting of the Nankai Trough and bathymetric map of drill sites. Site 1 (Tenryu) is in a sedimentary basin, Site 2 (Tokai) and Site 3 (Atsumi) are on the accretionary ridge. ODP Site 808 is located on the accretionary wedge in the southern part of the Nankai area.

intersected the subduction zone to the south of present-day Kyushu. This earlier configuration was changed about 20 Ma ago by the emplacement of the Philippine Sea Plate in this region (Taylor, 1992; Okino et al., 1994). The total thickness of the continental wedge in this region, i.e. the depth to the subducting slab, has been estimated to be between 10 and 15 km, depending on the distance to the trench. Hydrates are found on the continental side of the trough in sediments dominated by coarsely grained material with a substantial component derived from terrigenous sources (Kagami, 1985; Taira et al., 1992). BSRs have been identified at depths varying between 200 and 500 mbsf throughout most of the landward side of the Nankai Trough, suggesting a very wide-spread occurrence of gas hydrates in this area (Matsumoto, 2000). In several areas, particularly at the ridge settings, double BSRs have been observed. Based on their tectonic setting, gas hydrate fields have been subdivided into several categories, as demonstrated by the schematic cross section through the Nankai

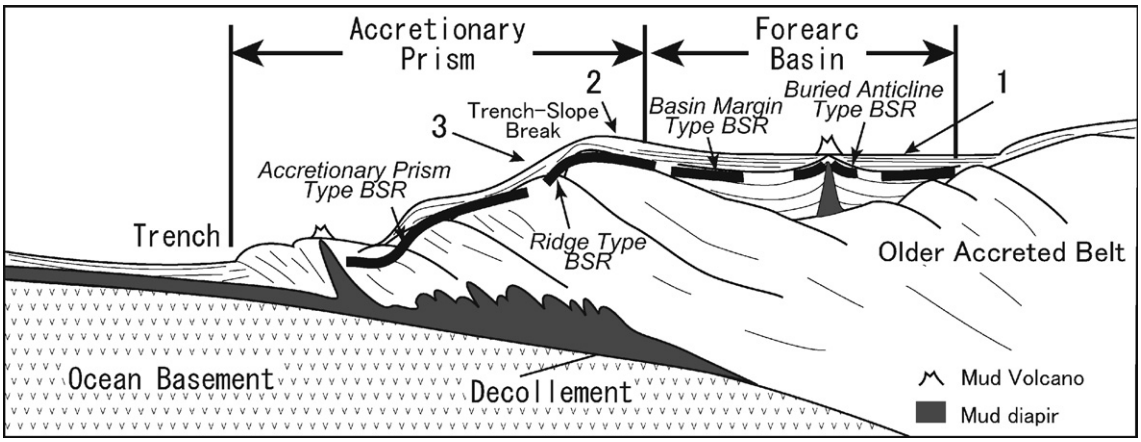

Fig. 2. Schematic cross section perpendicular to the Nankai Trough. Locations of the three drill sites are indicated with respect to sedimentary basin and accretionary wedge (after Baba and Yamada, 2004).

area (Fig. 2, Baba and Yamada, 2004). Although this categorization is simplified, it points to potential differences in the origin of CH_4 across the Nankai area.

The difference in tectonic settings is reflected in the age distribution of sediments present. The stratigraphy of the sedimentary basin is characterized by forearc and accretionary Cenozoic sediments (Tsuji et al., 2004; Uchida et al., 2004). The forearc sediments include the Mikura (Eocene to Oligocene), Kurami (Miocene), Saigo (Miocene), Sagara (Miocene to Pliocene), Kakegawa (Pliocene) and Ogasa (Pleistocene) groups in ascending order. Each of these formations is bounded by unconformities and consists of alternations of sandstone and siltstone with associated conglomerates and tuff. The accretionary sediments consist of the Setogawa (Eocene to Miocene), Ooigawa (Miocene), and Takakusayama (Miocene) groups, representing ocean-floor sediments and slope sediments including allochthonous limestone blocks.

The ridge and accretionary prism settings lack the older formations present in the sedimentary basin. ODP site 1178 probably is representative for a ridge location as those of Atsumi and Tokai (Shipboard Scientific Party, 2001), which indicates that no material older than mid-Miocene is present at ridge and accretionary wedge sites, reflecting the age of initiation of the current subduction situation at Nankai. Accretionary wedges typically contain numerous fractures, mostly trending parallel to the decollement, which are likely conduits for large scale dewatering of the accumulating sediments. Although specific information on the presence of fractures in this particular location is not available yet, it is very likely that fractures are also present in the accretionary ridge in this area.

Site 1, Tenryu: This drill site was part of a program organized by the Ministry of International Trade and Industry (MITI; now Ministry of Economy, Trade and Industry, METI). The actual drilling was carried out in 1999–2000, resulting in two pilot holes and one main hole, all close to 34°12′56″N and 137°45′02″E in the northeastern Nankai Trough area. Results from this program are published in a special issue of Resource Geology (Matsumoto et al., 2004a). The specific site is called Nankai Trough Site in this publication, but the authors will use Tenryu for the further discussion here, since all three sites were located in the Nankai Trough area. The drill site is located in the sedimentary basin formed between the current accretionary wedge and the old accretionery belt at a water depth of 945 m. The two pilot wells, BH1 and 2, reached depths of approximately 655 and 541 mbsf, respectively, the subsequently drilled main hole reached a depth of 678 m. The lower end of the hydrate stability zone in this region is indicated by two BSRs, a strong one at 263 mbsf, and a weaker one at 289 mbsf (Matsumoto et al., 2004b). Continuous coring was carried out through most of the hydrate stability zone. Samples of 51 pore water from these sites were received.

Site 2, Tokai: Sites 2 and 3 are part of the gas hydrate exploration program, METI/JOGMEC-MH21, carried out from January to May 2004, which included two deep drill sites in the Tokai area and the Atsumi area (see Figs. 1 and 2). Tokai is a ridge setting, located on the Dai-ichi Tenryu Knoll. Water depth is 720 m, and the drilling reached a

depth of about 250 mbsf. This site has a double BSR, one at 210 mbsf and the other at 245 mbsf. High resistivity values indicate strong presence of hydrate in a 100 m thick zone above the upper BSR (Takeuchi and Matsumoto, 2005). A total of 138 pore water samples from this core were available for this study, together with sediment squeeze cakes.

Site 3, Atsumi: This site is located on the northern flank of the Dai-ni Atsumi Knoll, at the transition between ridge and accretionary wedge. The water depth was 1006 m, the drilling reached a depth of about 400 mbsf. A single BSR was observed at a depth of 340 mbsf, but two separate high resistivity zones were recognized between 105–260 mbsf and 290–330 mbsf. The lower zone shows a stronger abnormality than the upper one, but neither one is as strong as those observed at Tokai or Tenryu. Approximately 100 pore water samples recovered from this site were used for this study. Iodine and Br concentrations were also determined in a subset of the associated sediment squeeze cakes.

3. Samples and methods

Pore water samples were taken during the drilling operation, squeezed from the recovered core material following established ODP protocol using Manheim type hydraulic squeezers. Actual samples sizes varied between 3 and 25 mL, less than 1 mL of which was used for the concentration measurements and diluted with 0.5% tetramethyl ammonium hydroxide (TMAH) solution by factors between 50 and 500, depending on the expected I concentration. TMAH, an organic alkaline solution, was used as a trap solution because it dissolves all I species. Iodine, Br and Cl concentrations for the Tokai and Atsumi samples were determined by ICP-MS, Agilent 7500 at Gakushuin University. Atomic masses used in the determinations were 127 for I, 79 for Br and 35 for Cl, respectively. In order to correct drift during the ICP-MS measurement, Cs was added as an internal standard to the solution (20 μg/L). Iodine and Br concentrations for the Tenryu site were determined at the ICP-MS system at NIRS, following the same protocol, while Cl concentrations for this set were measured at the ion chromatograph at Tokyo University. A subset of the concentration results for this site together with $^{129}I/I$ ratios was published in an earlier paper (Fehn et al., 2003).

For the analysis of sediment (solid phase), samples (0.2 g) were placed in a quartz tube and heated to 1000 °C under O_2 flow. Volatilized I and Br were collected in a trap solution containing TMAH (0.5%) and Na_2SO_3 (0.02%). Concentrations of I and Br were then determined by ICP-MS as for the pore water samples. Standard deviations of two or three determinations were less than 5%. Details of the analytical procedure were described in a previous paper (Muramatsu and Wedepohl, 1998). In addition to the measurement of I concentrations for the samples, I speciation (I^- and IO_3^-) was determined in selected pore water samples by ion chromatography coupled to the ICP-MS.

4. Results

Halogen concentrations in pore fluids (I, Br and Cl) and solid phases of the sediments (I and Br) for the three sites are listed in Tables 1–3; depth profiles for the three sites are shown in Figs. 3–5. In the analysis of sediment samples, squeezed cakes were used without further treatment. Concentrations of I and Br could be affected by the remaining pore fluids in the samples after squeezing. Since pore fluid contents have not been measured in each sample, no accurate corrections on the I concentrations in the solid phase of the sediments could be made. If the pore fluid contents are considered as 8% (in the case of Mackenzie samples studied by Tomaru, unpublished), contributions of I from the remaining pore fluid are estimated to be 20–40%. In other words, I and Br concentrations in the solid phase of the sediments are maximum values and might be about 30% lower than the measured values reported in the tables.

Starting with the results from Site 1, Tenryu (Fig. 3), Cl concentrations are close to the seawater concentration (seawater values are indicated by full circles at the upper margin in all panels) throughout the whole depth, except for some lower values just above the upper BSR. As is typical for many sites with gas hydrates present, I concentrations increase rapidly with depth from seawater values. The highest values of about 0.23 mmol/L (about 30 ppm) are reached at around 100 mbsf, a gradual decrease can be observed beyond this depth to values below 0.15 mmol/L. In addition, I values also show considerable fluctuation similar to the Cl set at depths just above the upper BSR. Only a limited set of samples was used for the determination of I concentrations in sediments in this core, but they display an

Table 1
Halogen concentrations in pore waters and sediments from Site 1, Tenryu

Depth (mbsf)	Pore water			Sediments (solid phase)		Porosity[a] [estimated] (%)	Sediments (total)[b]		Proportion in pore water	
	I (mmol/L)	Br (mmol/L)	Cl (mmol/L)	I (mmol/kg)	Br (mmol/kg)		I (mol/m^3)	Br (mol/m^3)	I (%)	Br (%)
0	0.0004	0.84	531			70.0				
0.4	0.0031	0.81		0.258	0.755	70.0	196	1137	1.1	50
21	0.102	0.97	542	0.187	0.626	68.9	216	1155	33	58
31	0.129	0.93	536			68.3			33	58
46	0.164	0.94	525	0.114	0.517	67.6	203	1058	54	60
61	0.187	0.96	533			66.8				
77	0.165	1.03	537			66.0				
90	0.215	0.99	529			65.3				
108	0.195	0.98	541			64.4				
120	0.233	1.04	537			63.8				
140	0.098	0.91				62.8				
150	0.205	1.00				62.4				
160	0.222	1.02	538			61.9				
162	0.194	0.99	542			61.8				
165	0.176	0.97	540			61.6				
174	0.215	1.00	529			61.2				
180	0.215	1.00	522			60.9				
184	0.180	0.98	547	0.087	0.300	60.8	195	893	56	67
202	0.053	0.56	346	0.030	0.243	59.9	62	579	51	58
217	0.198	0.99	527	0.143	0.477	59.2	264	1075	45	55
220	0.192	1.00	502			59.1				
222	0.187	0.96	548			59.0				
228	0.140	0.95	543			58.7				
231	0.032	0.42	254			58.6				
235	0.035	0.51	302			58.4				
237	0.128	0.97	475			58.3				
240	0.185	1.08	546			58.2				
240	0.046	0.76	490			58.2				
246	0.170	0.96	535			57.9				
249	0.067	0.86	518			57.8				
253	0.027	0.45	251			57.6				
253	0.024	0.41	251			57.6				
254	0.031	0.32	185	0.006	0.134	57.6	24	329	73	57

(*continued on next page*)

Table 1 (*continued*)

Depth (mbsf)	Pore water			Sediments (solid phase)		Porosity[a] [estimated] (%)	Sediments (total)[b]		Proportion in pore water	
	I (mmol/L)	Br (mmol/L)	Cl (mmol/L)	I (mmol/kg)	Br (mmol/kg)		I (mol/m^3)	Br (mol/m^3)	I (%)	Br (%)
255	0.033	0.41	230			57.5				
257	0.158	0.99	538			57.4				
260	0.013	0.71	387			57.3				
263	0.169	0.90	513			57.2				
264	0.081	0.50	528			57.1				
272	0.135	0.95	540			56.8				
289	0.128	0.91	542			56.0				
305	0.142	1.02	514	0.048	0.309	55.3	132	908	59	62
314	0.140	0.95	523			55.0				

[a] Porosity: assuming porosity values measured at Atsumi (upper sediment: 70%; bottom sediment at 314 m: 55%), the values at different depths were estimated by an exponential equation.
[b] Total concentrations of iodine and bromine were calculated for the sediments (including solid and fluid phases), using the porosity data and a constant density of 2.5 g/cm^3.

almost inverse profile with depth, with the highest values of 0.26 mmol/kg right at the surface and considerably lower values at depth. The Br concentrations in the pore waters show a behavior more similar to that of Cl than I, although the concentrations are generally higher than in seawater, except for depths just above the BSR, which also show considerable fluctuation. Bromine concentrations in sediments display an almost monotonous decrease with depth, with less variation than the I values.

The profiles for Site 2, the Tokai core (Fig. 4), show considerably more variation than the other two sites. Chlorine values increase from surface values close to seawater to values reaching 840 mmol/L (30,000 ppm) at 120 mbsf. Below this maximum, a gradual decrease is observed until they reach values close to seawater concentrations for the remaining profile. Starting at the depth of the maximum, very high values often alternate with very low values until the BSR is reached. The I profile shows an almost linear increase with depth from seawater values until it reaches a maximum close to 0.45 mmol/L at a depth of 125 mbsf. From this depth on, large fluctuations in the concentrations are visible, but even below the BSR I is still considerably enriched compared to seawater. Iodine concentrations in the sediments are quite low, generally below 0.1 mmol/kg and do not show a clear depth dependence. Bromine concentrations in the pore waters increase quite strongly with depth until they reach a maximum at the same depth as the profiles of Cl and I. Large fluctuations are visible in the Br profile similar to those of the other two profiles, but the Br values remain above seawater values even below the BSR. Bromine concentrations in the sediments are around 0.15 mmol/kg with, compared to the other two sites, relatively little variation throughout the core.

In terms of variability, the profiles for Site 3, Atsumi (Fig. 5), fall between those of the other two sites. Although most Cl concentrations are close to that of seawater, there are several groups of samples which have values above 600 mmol/L. Again, just above the BSR, many samples have concentrations considerably below seawater values. The Br values in the pore waters follow the general trend of the Cl concentrations, although most of them are again above seawater values, with the maxima just beyond 0.1 mmol/kg. The Br concentrations in the sediments are generally low and do not show a discernable pattern with depth. Iodine concentrations in

Table 2
Halogen concentrations in pore waters and sediments from Site 2, Tokai

Depth (mbsf)	Pore water			Sediments (solid phase)		Porosity[a] [estimated] (%)	Sediments (total)[b]		Proportion in pore water	
	I (mmol/L)	Br (mmol/L)	Cl (mmol/L)	I (mmol/kg)	Br (mmol/kg)		I (mol/m^3)	Br (mol/m^3)	I (%)	Br (%)
0	0.001	0.89	565	0.002	0.085	70.0	1.7	686	32	91
0.5	0.001	0.89	565			70.0				
1.5	0.002	0.89	570			69.9				
3	0.004	0.92	575	0.028	0.202	69.9	24	795	11	81
5	0.007	0.93	576			69.8				
6.5	0.011	0.94	570	0.028	0.178	69.7	29	790	26	83
8	0.015	0.09	582			69.6				
10	0.024	0.96	616	0.050	0.240	69.6	55	852	30	79
11.5	0.030	0.97	568			69.5				
13	0.039	0.98	573	0.020	0.170	69.4	42	814	64	84
14	0.045	1.00	576	0.016	0.166	69.4	43	823	72	85
14.5	0.046	0.95	574			69.4				
15	0.050	1.01	590			69.3				
15.5	0.051	0.97	584			69.3				
16.5	0.062	1.10	626			69.3				
16.9	0.057	0.98	592			69.3				
17.2	0.060	1.02	591	0.025	0.184	69.2	61	845	68	83
18	0.067	1.02	589			69.2				
18.5	0.069	1.01	608			69.2				
19	0.070	1.00	580	0.026	0.175	69.2	69	829	71	84
19.5	0.078	1.06	638			69.1				
20	0.077	1.02	589			69.1				
20.5	0.081	1.06	637			69.1				
21	0.081	1.03	586	0.014	0.104	69.1	67	790	84	90
21.5	0.083	1.04	612			69.1				
22	0.087	1.03	583			69.0				
22.5	0.091	1.06	634			69.0				
23	0.092	1.05	594			69.0				
23.7	0.098	1.12	676			69.0				
24	0.094	1.01	572	0.038	0.186	68.9	94	839	69	83
24.5	0.095	1.07	642			68.9				
25	0.097	1.09	651			68.9				
25.5	0.095	1.02	581			68.9				
26	0.095	1.07	642			68.9				
28	0.110	1.05	585	0.035	0.194	68.8	103	871	74	83
28.5	0.112	1.09	652			68.7				
29	0.108	1.04	581			68.7				
29.5	0.113	1.12	647			68.7				
30	0.117	1.06	584	0.035	0.146	68.7	108	841	75	86
30.5	0.100	1.08	633			68.7				
31	0.093	1.02	578			68.6				

(*continued on next page*)

Table 2 (*continued*)

Depth (mbsf)	Pore water			Sediments (solid phase)		Porosity[a] [estimated] (%)	Sediments (total)[b]		Proportion in pore water	
	I (mmol/L)	Br (mmol/L)	Cl (mmol/L)	I (mmol/kg)	Br (mmol/kg)		I (mol/m^3)	Br (mol/m^3)	I (%)	Br (%)
31.5	0.117	1.09	625			68.6				
32	0.117	1.06	581			68.6				
32.6	0.130	1.14	648			68.6				
33	0.136	1.19	680			68.6				
33.5	0.129	1.08	586	0.038	0.158	68.5	118	866	75	86
34	0.117	1.11	630			68.5				
34.5	0.128	1.09	586			68.5				
35	0.128	1.09	586			68.5				
35.3	0.135	1.14	662			68.5				
36	0.131	1.10	586	0.023	0.106	68.4	108	836	83	90
36.5	0.135	1.15	674			68.4				
37	0.125	1.08	579			68.4				
37.5	0.135	1.14	667			68.4				
38.2	0.143	1.12	587	0.023	0.105	68.3	115	847	84	90
38.5	0.149	1.15	655			68.3				
39	0.158	1.26	728			68.3				
43	0.124	1.09	583			68.1				
43.5	0.154	1.14	627			68.1				
44	0.156	1.13	593	0.033	0.153	68.1	133	892	80	86
44.5	0.163	1.16	621			68.1				
45	0.161	1.15	599			68.0				
45.5	0.171	1.20	650			68.0				
46	0.167	1.15	601	0.054	0.232	68.0	156	968	73	81
46.5	0.175	1.21	660			68.0				
47	0.169	1.16	605			67.9				
47.5	0.171	1.19	630			67.9				
48	0.163	1.16	604	0.080	0.254	67.9	174	989	63	79
52.6	0.186	1.19	609			67.7				
53	0.177	1.19	627			67.7				
53.5	0.180	1.18	609	0.093	0.263	67.7	197	1012	62	79
54	0.194	1.21	644			67.6				
54.5	0.181	1.17	633			67.6				
72.2	0.248	1.29	661	0.016	0.156	66.9	179	989	93	87
81.3	0.276	1.34	674			66.5				
91.3	0.250	1.30	679			66.1				
100.5	0.280	1.37	710	0.046	0.223	65.7	223	1090	82	82
100.8	0.046	0.51	308			65.7				
109.7	0.043	0.43	257	0.035	0.151	65.3	58	412	48	68
123.4	0.361	1.64	834			64.7				
125.6	0.447	1.78	841			64.7				
126	0.124	0.55	283	0.012	0.039	64.6	90	391	88	91
129.1	0.392	1.63	793			64.9				
129.6	0.154	0.63	314			64.5				

130.6	0.410	1.63	768	0.029	0.088	64.4	290	1130	91	93
138.4	0.348	1.54	758			64.1				
149.1	0.077	0.55	311			63.7				
149.6	0.410	1.62	755	0.070	0.234	63.7	325	1242	80	83
150	0.361	1.50	690			63.7				
157.2	0.221	1.16	576			63.4				
157.7	0.071	0.62	347	0.068	0.238	63.3	107	608	42	64
158.7	0.072	0.32	167			63.3				
159.4	0.341	1.39	644	0.007	0.064	63.3	222	939	97	94
162	0.283	1.28	610			63.2				
162.5	0.099	0.56	299			63.2				
163	0.109	0.52	268	0.053	0.193	63.1	117	506	59	65
163.5	0.302	1.20	558			63.1	117	506	59	65
163.7	0.189	1.04	528			63.1				
164	0.079	0.39	201	0.005	0.040	63.1	54	280	92	87
165.5	0.262	1.12	539			63.0				
165.9	0.284	1.15	535			63.0				
167	0.146	0.81	416	0.003	0.025	63.0	95	536	97	96
167.5	0.093	0.50	261			63.0				
168	0.058	0.35	189			62.9				
168.5	0.313	1.23	578	0.045	0.144	62.9	239	907	83	85
169	0.070	0.39	206			62.9				
169.4	0.303	1.19	565			62.9				
170.4	0.331	1.23	581	0.067	0.238	62.8	270	996	77	78
176.5	0.280	1.12	541			62.6				
177	0.220	0.90	453			62.6				
177.5	0.116	0.47	236	0.070	0.233	62.6	138	513	52	58
177.7	0.195	1.04	548			62.6				
178	0.091	0.44	235			62.5				
178.5	0.056	0.33	191	0.009	0.041	62.5	44	247	80	84
179	0.331	1.21	575			62.5				
186.5	0.266	1.11	560			62.2				
187.5	0.239	1.08	556	0.006	0.038	62.2	155	707	96	95
187.9	0.196	0.77	381			62.2				
188.1	0.302	1.12	535			62.1				
195	0.139	0.96	541	0.058	0.190	61.9	142	774	61	77
195.4	0.228	1.03	522			61.9				
196.1	0.091	0.41	211			61.8				
196.5	0.317	1.13	532	0.054	0.222	61.8	247	910	79	77
204.6	0.312	1.14	541			61.5				
204.7	0.258	1.13	566			61.5				
205.1	0.323	1.14	541			61.5				
205.5	0.339	1.19	540			61.5				
223.6	0.344	1.18	551	0.039	0.114	60.8	248	829	84	87
224	0.345	1.19	542			60.7				
224.5	0.194	1.03	547			60.7				

(*continued on next page*)

Table 2 (*continued*)

Depth (mbsf)	Pore water			Sediments (solid phase)		Porosity[a] [estimated] (%)	Sediments (total)[b]		Proportion in pore water	
	I (mmol/L)	Br (mmol/L)	Cl (mmol/L)	I (mmol/kg)	Br (mmol/kg)		I (mol/m^3)	Br (mol/m^3)	I (%)	Br (%)
228.7	0.318	1.15	540			60.6				
229	0.358	1.18	541			60.6				
233	0.204	1.05	541	0.072	0.021	60.4	195	884	63	75
233.7	0.345	1.18	566			60.4				
234	0.265	1.12	547			60.4				
242.5	0.306	1.14	562			60.0				
243	0.374	1.20	534			60.0				
243.4	0.380	1.21	558	0.050	0.223	60.0	278	948	82	77

[a] Porosity: one of the co-author (Takeuchi) determined porosity of upper sediment (70%) and bottom sediment at 243 m (60%) in this area. The values at different depths were estimated by an exponential equation using the upper and bottom values.
[b] Total concentrations of iodine and bromine were calculated for the sediments (including solid and fluid phases), using the porosity data and a constant density of 2.5 g/cm^3.

the pore waters increase very rapidly with depth to values higher than 0.35 mmol/L at a depth of 50 mbsf and remain high for most of the profile. Just above the BSR, I values decrease, however, very rapidly to values below 0.04 mmol/L with some variation similar to that observed for Cl and Br. Iodine concentrations in the sediments increase also from low surface values and reach a shallow maximum at 50 mbsf, decrease from that depth to values around 0.15 mmol/kg, but with considerable variation.

In selected samples from the hydrate sections of all three cores, I concentrations were determined also using ion chromatography (IC) coupled to ICP-MS. Using this system I^- and IO_3^- (if any) were separately determined. The results obtained by this system demonstrate that I is found almost exclusively in the form of I^- throughout the hydrate layers in these sites, an observation consistent with the anoxic environment in marine sediments below the SO_4 reduction depth.

5. Discussion

Major features in the concentration profiles common to the three sites are the strong enrichment in I, a less pronounced increase of Br with depth and considerable fluctuation in the concentrations of the three halogens in the layer close to the lower boundary of the hydrate stability zone, indicated by the upper BSR in the profiles. The profiles display, however, also major differences, particularly the shape of the I profiles, the presence of concentrations higher than seawater in two of the Cl profiles, particularly in the Tokai site, and the variations in the sediment concentration profiles.

5.1. Iodine enrichment

Iodine enrichment in pore waters has been observed in all marine sites where gas hydrates are present, such as Peru Margin (Martin et al., 1993), Blake Ridge (Egeberg and Dickens, 1999) and Hydrate Ridge (Fehn et al., 2006). This enrichment is related to the strongly biophilic behavior of I, which leads to a close association of this element with organic matter. While I is particularly strongly enriched in marine organic matter, it is generally released during the decomposition of organic matter, the source material for crude oils and natural gas. Investigations of crude oil have found very low concentrations of I in the oil itself, but consid-

Table 3
Halogen concentrations in pore waters and sediments from Site 3, Astumi

Depth (mbsf)	Pore water			Sediments (solid phase)		Porosity[a] [estimated] (%)	Sediments (total)[b]		Proportion in pore water	
	I (mmol/L)	Br (mmol/L)	Cl (mmol/L)	I (mmol/kg)	Br (mmol/kg)		I (mol/m^3)	Br (mol/m^3)	I (%)	Br (%)
0.3	0.001	0.89	561	0.002	0.085	70.0	1.7	686	32	91
5				0.069	0.212	69.8				
5.5				0.050	0.269	69.7				
6.5	0.121	1.01	584	0.110	0.267	69.7	168	906	50	78
12.5	0.330	1.43	755	0.115	0.283	69.4	317	1212	72	82
20	0.307	1.07	535	0.140	0.287	69.0	321	958	66	77
25.9	0.270	1.05	539	0.184	0.424	68.7	330	1050	56	68
32	0.354	1.11	549	0.182	0.323	68.4	386	1015	63	75
39.5	0.357	0.92	538	0.209	0.352	68.1	409	906	59	69
45.7	0.376	1.08	547	0.151	0.313	67.8	376	985	68	74
52.5	0.378	1.19	558			67.5				
59	0.376	1.16	544	0.194	0.328	67.1	412	1051	61	74
65.5	0.359	1.12	536	0.151	0.299	66.8	365	996	66	75
72.5	0.369	1.12	540	0.174	0.315	66.5	391	1007	63	74
78	0.391	1.24	558	0.183	0.293	66.2	413	1071	63	77
84	0.325	1.19	573	0.197	0.390	66.0	382	1117	56	70
92.5	0.339	1.16	559	0.126	0.265	65.6	331	990	67	77
102	0.345	1.28	645	0.124	0.234	65.1	332	1039	68	80
103.5	0.352	1.25	619			65.1				
105	0.335	1.18	569			65.0				
106.5	0.347	1.20	586	0.146	0.272	64.9	354	1015	64	77
108	0.350	1.20	600			64.9				
112.6	0.347	1.19	585			64.7				
117.6	0.313	1.13	579	0.124	0.295	64.4	313	988	65	73
120.6	0.339	1.15	584			64.3				
123.5	0.338	1.15	567			64.2				
125.5	0.356	1.15	568	0.101	0.237	64.1	319	951	72	78
127.3	0.351	1.15	567			64.0				
129.7	0.321	1.05	526			63.9				
130	0.323	1.03	501	0.083	0.219	63.9	281	858	73	77
135.9	0.332	1.05	504			63.6				
139	0.339	1.05	505	0.093	0.215	63.5	300	861	72	77
140.7	0.097	0.45	265	0.028	0.080	63.4	87	361	71	80
143.5	0.343	1.05	535	0.064	0.163	63.3	275	814	79	82
144	0.364	1.08	520	0.094	0.258	63.2	317	922	73	74
146.1	0.358	1.26	533	0.072	0.203	63.1	292	982	77	81
147.8	0.093	0.43	204	0.012	0.051	63.1	70	317	84	85
149.5	0.372	1.23	545	0.101	0.245	63.0	327	1002	72	77
151.6	0.346	1.14	524	0.095	0.267	62.9	306	963	71	74
154.1	0.354	1.06	518			62.8				

(*continued on next page*)

Table 3 (*continued*)

Depth (mbsf)	Pore water			Sediments (solid phase)		Porosity[a] [estimated] (%)	Sediments (total)[b]		Proportion in pore water	
	I (mmol/L)	Br (mmol/L)	Cl (mmol/L)	I (mmol/kg)	Br (mmol/kg)		I (mol/m^3)	Br (mol/m^3)	I (%)	Br (%)
154.7	0.369	1.16	526			62.8				
163.5	0.324	1.15	573			62.4				
165	0.353	1.15	515			62.3				
168.1	0.348	1.14	521			62.2				
168.5				0.078	0.196	62.1				
171	0.370	1.19	532	0.103	0.259	62.0	327	981	70	75
173	0.361	1.19	552			62.0				
175.6	0.359	1.20	563			61.8				
177.3	0.394	1.24	570	0.086	0.183	61.8	325	942	75	81
182.2	0.352	1.21	577			61.6				
183.1	0.360	1.21	568			61.5				
184.5	0.347	1.23	566	0.099	0.253	61.5	315	997	70	76
186	0.410	1.27	580	0.074	0.150	61.4	323	923	78	84
190.7	0.292	1.13	571	0.080	0.240	61.2	257	922	70	75
192	0.402	1.29	595	0.111	0.245	61.1	353	1026	69	77
199.5	0.389	1.25	587			60.8				
202	0.357	1.19	580			60.7				
209.5	0.405	1.26	594	0.098	0.227	60.4	341	987	72	77
211	0.408	1.28	601			60.3				
212.5	0.357	1.24	601			60.2				
214.2	0.373	1.24	591	0.042	0.119	60.2	266	863	84	86
234.9	0.352	1.21	568			59.3				
244	0.345	1.14	556			58.9				
244.3	0.350	1.18	578	0.093	0.229	58.9	301	930	68	75
246.9	0.327	1.26	532			58.6				
248.5	0.217	0.94	476	0.061	0.158	58.7	191	715	67	77
249	0.265	1.04	510			58.6				
250.6	0.337	1.11	532			58.6				
251.6	0.272	1.04	510			58.6				
256.2	0.334	1.16	566	0.028	0.066	58.4				
257.6	0.331	1.16	569			58.4				
261.9	0.305	1.14	579			58.2				

266	0.344	1.23	611	0.095	0.254	58.0	300	981	67	73
267	0.378	1.29	596			58.0				
268.5	0.353	1.25	608			57.9				
269.6	0.349	1.24	594	0.087	0.232	57.9	294	962	69	75
275.6	0.290	1.24	607			57.6				
276.7	0.372	1.24	607			57.6				
278	0.345	1.27	611	0.139	0.297	57.5	346	1046	57	70
280	0.258	1.21	594	0.087	0.232	57.9	294	962	69	75
282.8	0.264	1.25	616			57.3				
285.4	0.346	1.27	616			57.3				
287.7	0.367	1.31	626	0.134	0.323	57.1	353	1095	59	68
290.1	0.245	0.97	456	0.091	0.403	57.0	238	984	59	56
291	0.347	1.32	616	0.125	0.293	57.0	333	1065	60	70
294.9	0.152	0.69	336	0.076	0.138	56.8	168	538	51	72
295.9	0.142	0.62	303	0.094	0.153	56.8	182	518	44	68
297	0.113	0.59	300	0.067	0.126	56.8	137	473	47	71
298	0.243	1.16	637	0.155	0.476	56.7	305	1172	45	56
303.7	0.053	0.80	499	0.053	0.0244	56.5	87	720	34	63
305	0.128	0.88	486	0.038	0.190	56.4	113	702	64	70
307.2	0.109	0.71	405	0.011	0.073	56.4	74	480	84	83
310.8	0.214	0.95	499	0.061	0.180	56.2	187	733	64	73
314	0.175	0.84	451	0.039	0.119	56.1	141	600	69	78
315.5	0.175	0.84	454	0.046	0.174	56.0	149	660	66	71
323.6	0.026	0.53	334	0.008	0.111	55.7	23	420	62	71
324.9	0.088	0.64	376	0.036	0.136	55.7	89	510	55	70
326.4	0.130	0.71	400			55.6				
327.4	0.104	0.74	427			55.6				
332.4	0.033	0.55	340	0.009	0.119	55.4	29	439	63	70
334.7	0.044	0.55	340	0.009	0.119	55.3				
336.2	0.054	0.68	395			55.2				
341.7	0.110	0.90	519	0.024	0.146	55.0	88	661	69	75

[a] Porosity: one of the co-author (Takeuchi) determined porosity of upper sediment (70%) and bottom sediment at 341 m (55%) in this area. The values at different depths were estimated by an exponential equation using the upper and bottom values.

[b] Total concentrations of iodine and bromine were calculated for the sediments (including solid and fluid phases), using the porosity data and a constant density of 2.5 g/cm^3.

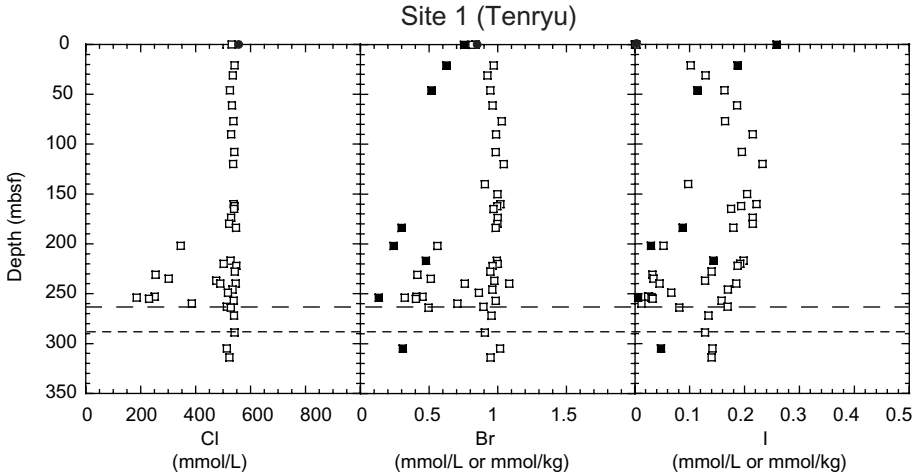

Fig. 3. Halogen profiles in pore waters (open squares) and sediments (closed squares) from Site 1 (Tenryu). The two broken lines indicate BSRs at 263 and 289 mbsf, respectively. Closed circles show seawater concentrations (GERM, 2006).

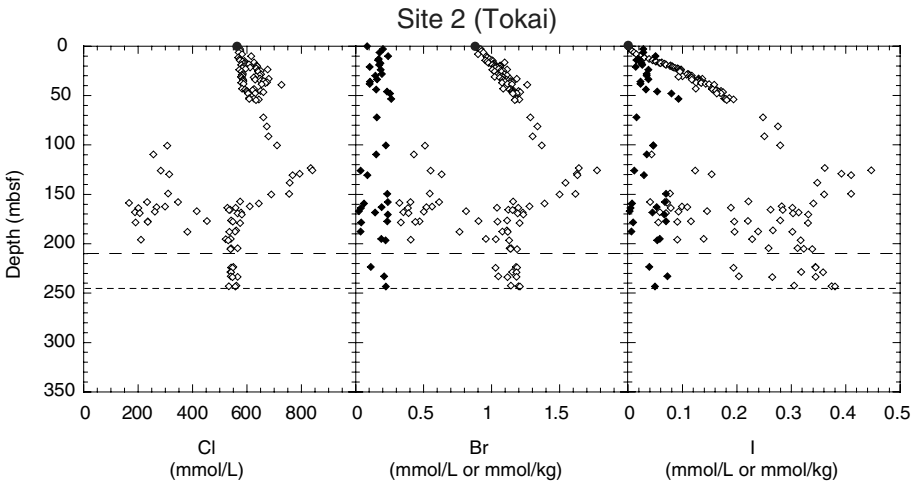

Fig. 4. Halogen profiles in pore waters (open diamonds) and sediments (closed diamonds) from Site 2 (Tokai). The BSRs are at 210 and 245 mbsf. Closed circles show seawater concentrations (GERM, 2006).

erable enrichment in oil field brines and similar aquatic fluids (Fehn et al., 1990; Moran et al., 1995). The degree of enrichment observed in the three Nankai cores is lower than in the other sites mentioned here. While the general enrichment in I in these cores is thus not surprising, the shape of the profiles, in particular the large fluctuation in values just above the BSR has so far not been observed in other profiles and needs further discussion.

5.2. Variability in concentrations

All profiles display considerable variability in the layer above the upper BSR. This behavior is commonly observed in Cl profiles in other marine gas hydrate locations (Egeberg and Dickens, 1999; Fehn et al., 2006). It is related to the dissociation of gas hydrates and the accompanying dilution of pore waters by fresh water. The profiles presented here are, however, the first examples where this behavior is also observed in the Br and I concentrations. Since the strongest variability is observed in the Tokai core, this core is used for a closer look at this question with a close-up of the three profiles for the depth range between 150 and 200 mbsf shown in Fig. 6. An alternation between high and low values is visible, most clearly displayed in the segments where samples were spaced less than 1 m apart. The general pattern is identical for the three halogens in these

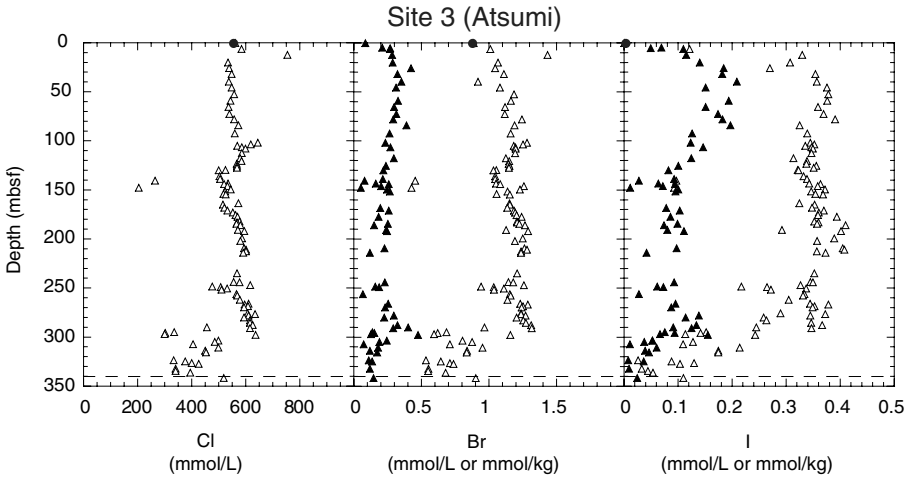

Fig. 5. Halogen profiles in pore waters (open triangles) and sediments (closed triangles) from Site 3 (Atsumi). Only a single BSR has been identified here, at 340 mbsf. Closed circles show seawater concentrations (GERM, 2006).

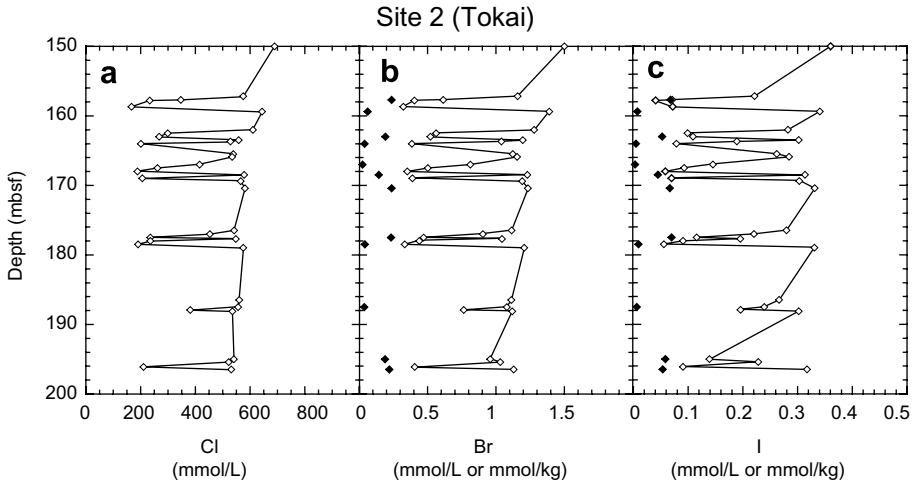

Fig. 6. Close-up of halogen profiles for depth range between 150 and 200 mbsf from Site 2 (Tokai). Symbols as in Fig. 4.

profiles, suggesting that the variation in concentration is caused by the same process. The comparison between sediment values and pore water concentrations for Br and I indicates at most a low degree of parallel behavior in these sections.

The most likely process responsible for the zigzag pattern observed in the concentration profiles is the freshening of pore waters due to the dissociation of gas hydrates, an accepted explanation for the fluctuation observed commonly in Cl profiles of gas hydrate sites. The presence of similar patterns in the two other profiles has not been observed in other sites, but allows testing of this assumption. Generally, the assumption is made that other ions are excluded during the formation of gas hydrates and that the melting of hydrate crystals releases essentially fresh water. If that were the case, dilution of pore waters should preserve the ratios between the three halogens. If the ratios are plotted for the three halogens, a zigzag pattern is, however, still clearly visible, very pronounced for I/Cl and I/Br, but almost absent for Br/Cl (Fig. 7), indicating that the dilution is not working at the same rate for the three elements. This observation can be explained if halogens are present at low, but different levels in gas hydrates. Solid gas hydrates were not recovered from any of the Nankai sites, but the concentrations of Cl, Br and I were determined in four solid gas

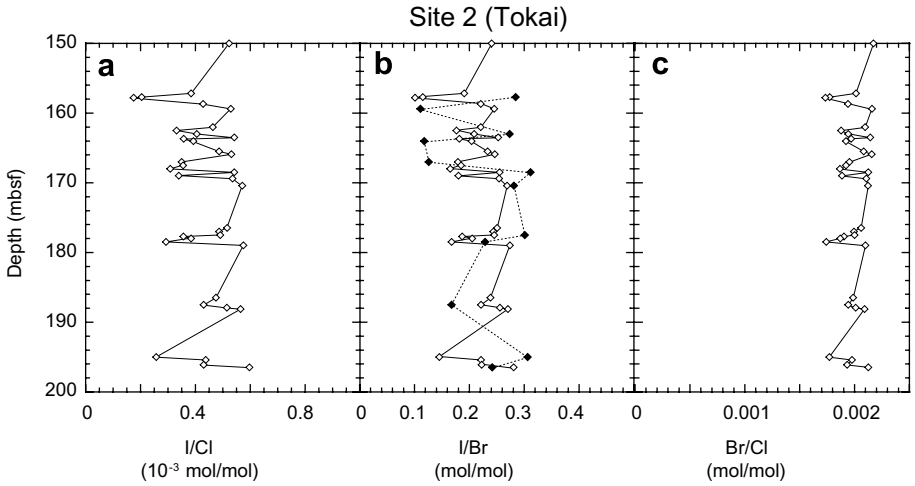

Fig. 7. Halogen ratios for depth range between 150 and 200 mbsf from Site 2 (Tokai). Symbols as in Fig. 4.

hydrate samples from the recent expedition to the Sado area in the Sea of Japan (Tomaru et al., 2007). The average concentrations for these four samples were 62.5 mmol/L Cl, 0.14 mmol/L Br and 0.00055 mmol/L I, indicating that small amounts of halogens are incorporated into gas hydrate crystals. If these concentrations are compared to the high concentrations in the core (Cl = 590 mmol/L; Br = 1.3 mmol/L; I = 0.31 mmol/L), ratios between pore water and gas hydrates concentrations for Cl and Br are close to 10, but are greater than 500 for I. The release of 'fresh' water from gas hydrates therefore dilutes pore water more strongly for I than for the other two halogens, reflected in the strong variability in the I/Cl and I/Br ratios, which is absent in the Br/Cl ratios. The relatively large ionic radius of I prevents this element from being incorporated into common minerals and is also the probable cause for the relatively low rate of uptake by gas hydrate crystals compared to the other two halogens. The comparison of I/Br ratios in sediments and pore waters (Fig. 7b) shows that values in both records vary quite strongly, but that the variation is largely independent of each other.

5.3. Concentrations of I and Br in sediments

The profiles for I and Br concentrations in sediments of the three cores show considerable differences. In Site 1 (Tenryu), high concentrations in the surface layers decrease quickly to considerably lower values at depth (see Fig. 3). This behavior has been observed in other sediment cores (e.g. Kennedy and Elderfield, 1987) and is caused by the input of organic material from the surface and release of these two elements back into the water column following the decomposition of organic material (e.g. Ullmann and Aller, 1980). The two elements follow a similar pattern, although variations in the I concentrations are larger than for Br, reflecting the close association of I with organic material. Although there is some degree of fluctuation in the concentrations at the lower end of the hydrate stability zone, there is no apparent correlation between concentrations in sediments and pore waters.

For site 2 (Tokai), I and Br concentrations fall into relatively narrow ranges and do not show the enrichment close to the surface found at Tenryu. There is more data for this core than for Site 1 and the results for pore waters and sediments can be compared for a large data set (Fig. 8). No apparent co-variation is visible in this case suggesting that the presence of I in pore waters and sediments originated from different sources.

A somewhat stronger case for co-variation can perhaps be made for Site 3, Atsumi (Fig. 9). A closer look suggests, however, that two populations of sediment values are present in this core, roughly separated at about 120 mbsf, with the shallower sediments containing more I than the deeper ones. As in the other two sites, it is therefore not very likely that pore waters in the gas hydrate layer reflect the presence of I (or Br) in the sediments and that these elements are derived from sources outside of the immediate area gas hydrates are found in.

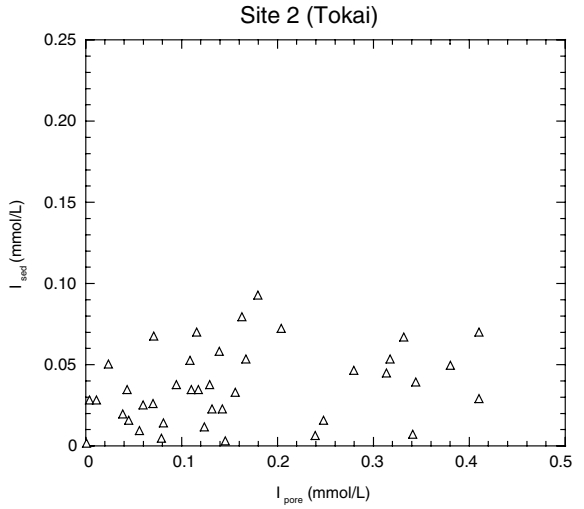

Fig. 8. Comparison of I concentrations in sediments and pore waters from Site 2 (Tokai).

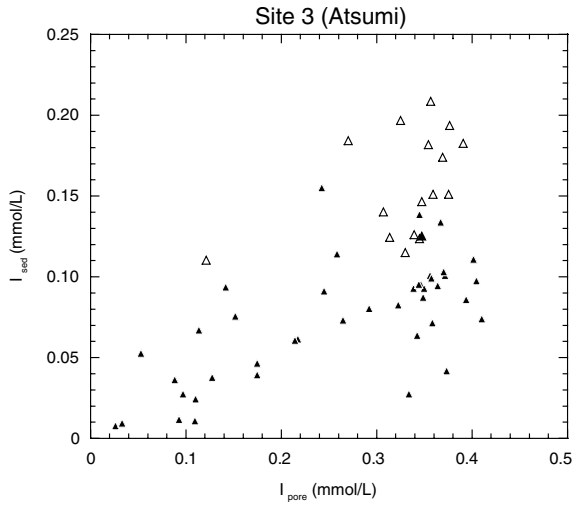

Fig. 9. Comparison of I concentrations in sediments and pore waters from Site 3 (Atsumi). Open triangles, samples above 120 mbsf; closed triangles, samples below 120 mbsf.

5.4. Interpretation of the halogen profiles

The halogen profiles for Site 1 (Tenryu) are quite similar to profiles found in other gas hydrate locations (Fehn et al., 2000; Fehn et al., 2006). Iodine shows a slight maximum at 120 mbsf, but values are still elevated below the two BSRs. The overall enrichment in I and Br is lower than in the other two Nankai sites. The comparison between I values in sediments and pore waters argues against derivation of I from local sediments. The profile thus suggests influx of fluids carrying I from below. Both of the other two profiles are consistent with such an interpretation. The quite smooth continuation of all three profiles at this site beyond the lower limit of the gas hydrate stability zone suggests that this transport continues for some distance beyond the area of study. In a subset of samples from this core $^{129}I/I$ ratios were determined which indicate that the source formation for the I in this location is older than 40 Ma (Fehn et al., 2003). Potential source formations of Early Eocene age are present in the deeper parts of the sedimentary basin where this core was taken. The likely derivation of I and, by association, of the CH_4 in the gas hydrate occurrences is thus from formations of Early Eocene age and includes the transport in aqueous fluids over distances of 1–5 km.

The profiles for the other two sites indicate that the situation there is quite different from that at the Tenryu site. At Site 2, the increase for I with depth, typical for many gas hydrate sites, is accompanied not only by a similar increase in Br, but also in Cl, until all three elements reach maximum values at 130 mbsf. These maxima are found just above the main layer of gas hydrates, indicated by the strong fluctuation of values discussed earlier. While elevated concentrations for I and Br are common in gas hydrate sites, the increase in Cl concentrations is unusual. These high concentrations might suggest the in situ formation of gas hydrates which is associated with the exclusion of Cl from the gas hydrate crystals and the subsequent enrichment of Cl in the associated pore waters. It is worth noting that the interval containing the maximum also contains samples with very low concentrations. It is likely that the closely spaced sampling in this core might have enabled distinguishing between adjoining samples, one containing gas hydrates which yield low concentrations upon dissociation, and the next being void of hydrates where pore waters have been enriched in halogens due to the exclusion from gas hydrate formation in the vicinity. The layer above the BSR therefore reflects complicated interactions between formation and dissociation of the gas hydrates, which, because of the relatively close sampling, can be observed here while in sampling from larger intervals probably would have produced a sample set with concentrations averaging the high and low values. The continuation of the profiles below the upper BSR indicates that, similar to Site 1, fluids with high concentrations of I enter this site from deeper layers. The overall concentrations in I are higher than in Site 1, but the more pronounced

maximum in this site suggests also, that there is an important lateral component of flow transporting I (and CH_4) into the hydrate layer. Because I dating at this site has not been carried out, potential source formations in this case have not been identified yet.

The very rapid increase in I concentrations at Site 3 (Atsumi) suggests that two different processes might be active in this case. The layers to about 50 mbsf show a parallel increase in I concentrations of pore water and sediments. Since gas hydrates are not present at that depth, these processes probably are not directly related to the formation of hydrates but reflect the presence of material with relatively high concentrations of organic material in this site close to the crest of the accretionary ridge. Below this layer, the I concentrations reach a maximum at about 200 mbsf, reasonably similar to the other two sites, but then decrease very sharply to values almost as low as seawater at depths close to and below the BSR. In contrast to the other two sites, this site does not indicate significant flow from below, but must have mostly lateral flow supplying the gas hydrate layer. The position of the site close to the ridge crest in an area, which probably contains multiple fractures supports this interpretation of the I profile. Iodine isotope measurements are planned which might allow the identification of potential source formations in this case as well.

Total I concentrations in the sediment (solids and pore fluids) can be estimated by using data for porosity, density and the measured values of I in pore waters and solid phase of the sediments. For porosity data of Tokai and Atsumi samples, the following values we used were determined by R. Takeuchi (unpublished):

Tokai: Upper sediment: 70%, at 243 m: 60%,
Atsumi: Upper sediment: 70%, at 341 m: 55%.

The porosities at different depth were estimated by an exponential equation using the above-mentioned upper and bottom values. Since no porosity data is available for Tenryu, the values from Atsumi were used here as well. The estimated porosities are shown in Tables 1–3 together with the concentration data. Specific values for densities were not determined, but the range for sediment densities is typically between 2200 and 2800 kg/m^3 (Snyder et al., submitted for publication) and, for the estimate of total I and Br concentrations, a density of 2500 kg/m^3 was assumed for the dry sediments. The estimated I and Br concentrations (mol/m^3) as well as the proportions of I and Br present in the pore fluids at each depth are listed in Tables 1–3. Excluding surface samples, the proportions of I in pore fluids collected from Tenryu, Tokai and Atsumi were around 60%, 80%, 70%, respectively. If the elevated I concentrations (up to 30%) in the squeezed samples are considered due to be used the remaining pore fluid as mentioned above, the actual proportion of I in the fluid phase probably is higher than these values.

The organic C (TOC) contents in the sediments of Nankai Trough are about 0.5% and they are relatively constant from the top to the bottom (Waseda and Uchida, 2004). These low organic C contents and the measured low I concentrations in the surface sediment layers suggest that the deposition rate of organic material is quite low in this area. It is also possible that I and C precipitated in surface sediments is dissolved and transported back into the overlying seawater by the decomposition of organic materials, resulting in the observed low I and organic C contents in sediments. In samples collected from Tokai and Atsumi, no particular accumulation of I was found in the surface layers. In the Tenryu samples, some accumulation of I was observed in the surface sediments, suggesting that I might be partially desorbed from the sediments and retained in the oxic layer of the top sediments. These results indicate that the observed high I concentrations in the pore fluids can not fully be explained by the in situ release of I from the sediments into the pore waters and necessitate consideration of pathways for I from other layers into the gas hydrate zone.

5.5. A model for the origin of gas hydrates in the Nankai area

The three sites are located at quite different geologic settings, allowing a general assessment of the formation of gas hydrates in this area. The comparison between sedimentary concentrations and pore water profiles speaks strongly against a direct derivation of I and Br from local sediments. This finding is in good agreement with mass balance considerations and the distribution of gas hydrates in different parts of active margins, which generally does not follow patterns of organic productivity. Since I and Br are not derived from local sources, they must be transported into their current location by aqueous fluids. This transport mechanism is likely also open to CH_4, which has very similar diffusion coefficients (CRC Handbook, 2004), as I^-,

the dominant species of I in the gas hydrate layers. The three sites suggest different modes of fluid transport in this area. The profile in Site 1 (Tenryu) is most compatible with advection from below as the most dominant transport mode there. The location at the top of a sedimentary basin is compatible with a model where fluids are moved upwards, following the pressure gradient induced by compaction. Iodine dating at this site has suggested that the main source formations are layers of Eocene age in the deeper parts of the basin (Fehn et al., 2003).

The concentration profiles of the other two sites near the top of the accretionary ridge display a distinctly different shape which suggests the presence of at least a strong component of lateral flow in both of these locations. The strong maximum in the profile at Site 3 (Atsumi) together with the return of the I and Br concentrations almost to seawater values at the BSR indicates that waters below the hydrate stability zone contain relatively little extra I and Br and probably also lack CH_4. The supply of CH_4 in this case therefore is likely to come mostly through lateral flow. Fractures are found frequently in accretionary wedges, typically with shallow dips following roughly that of the decollement, so that large scale lateral flow can easily be envisioned within accretionary wedges, as shown in flow models of subduction zones (Saffer and Bekins, 1998; Saffer and Bekins, 2002). The driving force in this case is a combination of compaction and seismic pumping, with flow directions generally from the landward side of the subduction zone towards the elevated parts of the accretionary wedge. In the given case, then, the source formation for I, Br and CH_4 is likely towards the landward side of the accretionary ridge. In the case of Site 3, this is probably the dominant source of these compounds, with minor additions possible from local sources. At Site 2 (Tokai), a mixture of lateral flow and advection from depth probably is responsible for the observed concentration profiles. A more specific identification of potential source locations will be possible once I isotope data are available for these sites as well.

5.6. Comparison to other gas hydrate sites

While numerous gas hydrate sites have been investigated recently, I and Br concentrations are available only from a relatively small subset of these sites. Data are available from Blake Ridge (ODP Leg 164; Egeberg and Dickens, 1999), Peru Margin (ODP Leg 201; Fehn et al., in press) and Hydrate Ridge (ODP Leg 204; Fehn et al., 2006). All of these sites have in common a strong enrichment in I found in the pore waters associated with gas hydrate occurrences, accompanied by an enrichment of Br, although to a much lesser degree. Chlorine concentrations are typically close to seawater values, although there are several sites where Cl concentrations decrease with depth (e.g. Blake Ridge; some sites at Hydrate Ridge). Iodine concentrations at the Nankai sites are considerably lower than those found in the other sites. A comparison of the maximum values found in individual drill cores from all these sites demonstrates this observation (Fig. 10). While maximum I concentrations in Nankai are between 0.2 and 0.4 mmol/L, they reach 1.2 mmol/L at Peru Margin and values above 1.6 mmol/L both in Blake Ridge and Hydrate Ridge. The considerably higher degree of enrichment both in I and Br is obvious in a comparison between I/Cl and Br/Cl ratios for these sites (Fig. 11). In this figure, the Nankai sites are relatively close to the seawater values, while sites from Hydrate Ridge and Blake Ridge show very strong enrichment.

Most of the I profiles taken at other sites are similar to that from Site 1 (Tenryu), i.e. a relatively rapid increase in I concentrations at shallow levels followed by rather constant values at depth. In all of the sites investigated so far, I concentrations remain elevated even below the hydrate stability limit, indicating steady flow of I-rich fluids from below. A few flank sites at Hydrate Ridge display more or less pronounced maxima in the I concentration at depth.

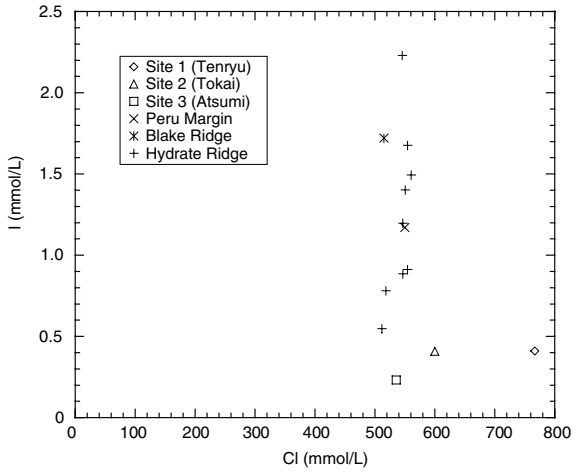

Fig. 10. Iodine maxima versus Cl concentration in the three Nankai Sites (this study) and those of Site 1230 (Peru Margin; Fehn et al., in press), Blake Ridge (Fehn et al., 2000) and nine sites from ODP Leg 204 (Hydrate Ridge; Fehn et al., 2006).

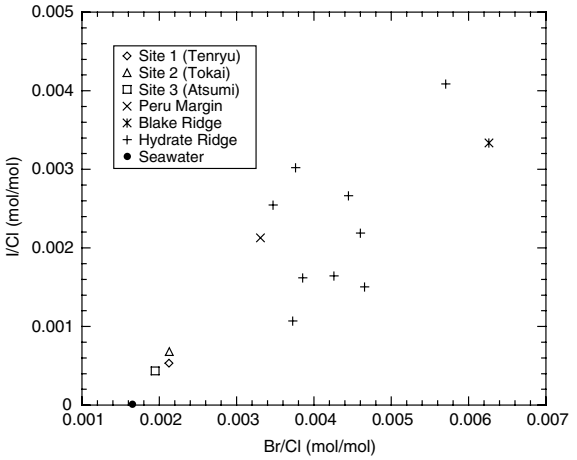

Fig. 11. I/Cl versus Br/Cl ratios for I maxima from the three Nankai Sites and those of Site 1230 (Peru Margin; Fehn et al., in press), Blake Ridge (Fehn et al., 2000) and nine sites from ODP Leg 204 (Hydrate Ridge; Fehn et al., 2006). Seawater values (GERM, 2006) are indicated by the closed circle.

A $^{129}I/I$ investigation of one of those sites (Site 1245) indicated that the cause of the maximum there is the mixing of I from two sources, one of Eocene and one of Pliocene age. It will be interesting to see whether the maxima in the Nankai Sites are also related to the mixing of material from two or more sources.

6. Conclusions

Halogen concentrations in closely spaced samples of pore waters and sediments from three deep drill cores taken in the northeastern region of the Nankai Trough Area are reported here. Site 1 (Tenryu) is located in the sedimentary basin separating the currently active accretionary wedge from an older accreted belt, while the other two sites are close to the crest of the active accretionary ridge. All three sites have at least one BSR, indicating the presence of gas hydrates in the respective locations. The profiles show a distinct increase in I concentrations with depth, accompanied by a somewhat lesser increase in Br concentrations. A comparison between results from IC and ICP-MS determinations indicates that I is found almost exclusively in the form of I^- throughout the gas hydrate layers. The highest I concentrations varied between 0.2 mmol/L (Site 1) and just above 0.4 mmol/L for the other two sites. While these concentrations constitute an increase by factors up to 1000 above seawater values, they are considerably lower than concentrations observed in other gas hydrate locations such as Hydrate Ridge and Blake Ridge. All three sites display large concentration fluctuations in the layer just above the BSR. Fluctuations of this kind are frequently observed in Cl profiles and are explained as the dilution caused by the dissociation of hydrates. For the first time here, they are documented also in I and Br profiles. The presence of fluctuations in element ratios of the three halides demonstrates that gas hydrates incorporate small amounts of halogen ions at rates decreasing from Cl to I.

I and Br concentrations in pore fluids and associated sediments follow different trends, which demonstrate that these two elements are not derived locally but are transported into their present location from other source formations. Because of the close association between organic material and I and the similarity of transport behavior for I^- and CH_4, the observation that I and Br are transported by aqueous fluids into young sediments allows the extrapolation, that CH_4 in the gas hydrate fields originated from the same source as these two elements. At Site 1 (Tenryu), the I profile suggests that vertical advection of fluids is mostly responsible for the supply of I, Br and CH_4. In contrast, the strong maximum of I concentrations at Site 3 (Atsumi) in the gas hydrate layer and the decrease in concentrations to values close to seawater below the BSR indicates a dominance of lateral flow in this location. The I profile at Site 2 (Tokai) falls in between these two cases and might be the consequence of mixing between lateral and horizontal flows. The difference in flow systematics agrees well with the location of Site 1 in a sedimentary basin and the two other sites at the currently active accretionary wedge.

Acknowledgements

We appreciate the use of samples collected during the methane hydrate project, MH21, of the Japan Oil, Gas and Metals National Corporation (JOGMEC) and the Ministry of Economy, Trade and Industry (METI) and thank Zunli Lu for help in the preparation of the manuscript. The paper benefited from thoughtful reviews by J. Gieskes, J. Martin and an anonymous reviewer, and from comments by G. Snyder and J. Moran, the guest editors of this issue. Research on this project was supported, by a Grant-in-Aid for Exploratory Research (MEXT, Japan) to YM, by a JSPS Post-Doctoral Fellowship for Research Abroad to HT and by NSF grant OCE-0550122 to UF.

References

Baba, K., Yamada, Y., 2004. BSRs and associated reflections as an indicator of gas hydrate and free gas accumulation: an example of accretionary prism and forearc basin system along the Nankai Trough, off Central Japan. Resource Geol. 54, 11–24.

CRC Handbook for Chemistry and Physics, 2004, 85th ed. CRC Press, New York.

Dickens, G.R., 2001. Modeling the global carbon cycle with a gas hydrate capacitor: significance for the latest Paleocene thermal maximum. In: Paull, C.K., Dillon, W.P. (Eds.), Natural Gas Hydrates: Occurrence, Distribution and Detection. Geophysics Monograph 124, pp. 19–38.

Dickens, G.R., Castillo, M.M., Walker, J.C.G., 1997. A blast of gas in the latest Paleogene: simulating first-order effects of massive dissociation of oceanic methane hydrate. Geology 25, 259–262.

Egeberg, P.K., Dickens, G.R., 1999. Thermodynamic and pore water halogen constraints on gas hydrate distribution at ODP Site 997 (Blake Ridge). Chem. Geol. 153, 53–79.

Fehn, U., Tullai-Fitzpatrick, S., Teng, R.T.D., Gove, H.E., Kubik, P.W., Sharma, P., Elmore, D., 1990. Dating of oil field brines using ^{129}I. Nucl. Instrum. Methods B52, 446–450.

Fehn, U., Snyder, G., Egeberg, P.K., 2000. Dating of pore waters with ^{129}I: relevance for the origin of marine gas hydrates. Science 289, 2332–2335.

Fehn, U., Snyder, G.T., Matsumoto, R., Muramatsu, Y., Tomaru, H., 2003. Iodine dating of pore waters associated with gas hydrates in the Nankai area, Japan. Geology 31, 521–524.

Fehn, U., Lu, Z., Tomaru, H., 2006. Data report: ^{129}I/I ratios and halogen concentrations in pore waters of the Hydrate Ridge and their relevance for the origin of gas hydrates: a progress report. In: Proceedings of ODP, Sci. Results 204, pp. 1–25, MS 204SR-107.

Fehn, U., Snyder, G.T., Muramatsu, Y., in press. Iodine as a tracer of organic material: ^{129}I results from gas hydrate systems and fore arc fluids. J. Geochem. Explor.

GERM, 2006. Geochemical Earth Reference Model. www.earthref.org/GERM.

Hyndman, R.D., Foucher, J.P., Yamano, M., Fisher, A.Scientific Team of Ocean Drilling Program Leg 131, 1992. Deep sea bottom-simulating-reflectors: calibration of the base of the hydrate stability field as used for heat flow estimates. Earth Planet. Sci. Lett. 109, 289–301.

Jarrard, R.D., 1986. Relations among subduction parameters. Rev. Geophys. 24, 217–284.

Kagami, H., 1985. Internal structures of the accretionary wedge in the Nankai Trough off Shikoku, southwestern Japan. In: Nasu, N., Kobayashi, K., Uyeda, S., Kushiro, I., Kagami, H. (Eds.), Formation of Active Ocean Margins. Terra Si. Publ., Tokyo, pp. 93–219.

Kastner, M., 2001. Ingerson lecture; Methane hydrates characterization and role in past and future climate change. GSA, Abstracts with Programs 33(6), pp. 189.

Kennedy, H.A., Elderfield, H., 1987. Iodine diagenesis in pelagic deep-sea sediments. Geochim. Cosmochim. Acta 51, 2489–2504.

Kennett, J.P., Cannariato, K.G., Hendy, I.L., Behl, R.J., 2003. Methane Hydrates in Quaternary Climate Change. Am. Geophys. Union, Washington, DC.

Kvenvolden, K.A., 1999. Potential effects of gas hydrate on humane welfare. Proc. Natl. Acad. Sci. USA 96, 3420–3426.

Martin, J.B., 1999. Non-conservative behavior of Br/Cl ratios during alteration of volcaniclastic sediments. Geochim. Cosmochim. Acta 63, 383–391.

Martin, J.B., Gieskes, J.M., Torres, M., Kastner, M., 1993. Bromine and iodine in Peru Margin sediments and pore fluids: implications for fluid origins. Geochim. Cosmochim. Acta 57, 4377–4389.

Matsumoto, R., 2000. Methane hydrate estimates from the chloride and oxygen isotopic anomalies – examples from the Blake Ridge and Nankai Trough sediments. Ann. New York Acad. Sci. 912, 39–50.

Matsumoto, R., Matsumoto, R., Uchida, T., Waseda, A., Shikazono, N., Aoki, Y., Tsuji, Y., 2004a. Gas Hydrate in Nankai Trough. Resource Geol. 54, 1–135.

Matsumoto, R., Tomaru, H., Lu, H., 2004b. Detection and evaluation of gas hydrates in the Eastern Nankai Trough by geochemical and geophysical methods. Resource Geol. 54, 53–68.

Milkov, A.V., Sassen, R., Apanasovich, T.V., Dadashev, F.G., 2003. Global gas flux from mud volcanoes: a significant source of fossil methane in the atmosphere and ocean. Geophys. Res. Lett. 30 (B2). doi:10.1029/2002GL016358.

Moran, J.E., Fehn, U., Hanor, J.S., 1995. Determination of source ages and migration patterns of brines from the U.S. Gulf Coast Basin using ^{129}I. Geochim. Cosmochim. Acta 59, 5055–5069.

Muramatsu, Y., Wedepohl, K.H., 1998. The distribution of iodine in the earth's crust. Chem. Geol. 147, 201–216.

Okino, K., Shimakawa, Y., Nagaoka, S., 1994. Evolution of the Shikoku Basin. J. Geomagn. Geoelectr. 46, 463–479.

Saffer, D.M., Bekins, B.A., 1998. Episodic fluid flow in the Nankai accretionary complex: timescale, geochemistry, flow rates, and fluid budget. J. Geophys. Res. 103, 30351–30370.

Saffer, D.M., Bekins, B.A., 2002. Hydrologic controls on the morphology and mechanics of accretionary wedges. Geology 30, 271–274.

Shipboard Scientific Party, 2001. Leg 190 summary. In: Moore, G.F., Taira, A., Klaus, A., et al. (Eds.), Proceedings of ODP, Initial Reports 190, pp. 1–87.

Sloan, E.D., 1998. Clathrate Hydrates of Natural Gases. Dekker, New York.

Snyder, G., Fehn, U., Dickens, G., submitted for publication. Iodine in open ocean and continental margin sedimentary sequences: dynamic cycling and accumulation on the sea floor. Earth Planet. Sci. Lett.

Taira, A., Hill, I., Firth, J., Berner, U., Brückmann, W., Byrne, T., Chabernaud, T., Fisher, A., Foucher, J.–P., Gamo, T., Gieskes, J., Hyndman, R., Karig, D., Kastner, M., Kato, Y., Lallemant, S., Lu, R., Maltman, A., Moore, G., Moran, K., Olaffson, G., Owens, W., Pickering, K., Siena, F., Taylor, E., Underwood, M., Wilkinson, C., Yamano, M., Zhang, J., 1992. Sediment deformation and hydrogeology of the Nankai Trough accretionary prism: synthesis of shipboard results of ODP Leg 131. Earth Planet. Sci. Lett. 109, 431–450.

Takeuchi, R., Matsumoto, R., 2005. Geochemistry of interstitial water in the Nankai Trough, South Japan. In: Proceedings of Fifth International Conference on Gas Hydrates, ICGH5, pp. 908–912.

Taylor, B., 1992. In: Rifting and the volcanic–tectonic evolution of the Izu-Bonin-Mariana Arc: Proceedings of Ocean Drilling Program, Scientific Results 126, pp. 627–651.

Tomaru, H., Lu, Z., Snyder, G., Fehn, U., Hiruta, A., Matsumoto, R., 2007. Origin and flow of pore waters in an actively venting gas hydrate field near Sado Island, Japan Sea: interpretation of halogen and ^{129}I distributions. Chem. Geol.

Tsuji, Y., Ishida, H., Nakamizu, M., Matsumoto, R., Shimizu, S., 2004. Overview of the MITI Nankai Trough wells: a milestone in the evaluation of methane hydrate resources. Resource Geol. 54, 3–10.

Uchida, T., Lu, H., Tomal, H.The MITI Nankai Trough Shipboard Scientists, 2004. Subsurface occurrence of gas hydrate in the Nankai Trough Area: implication for gas hydrate concentration. Resource Geol. 54, 35–44.

Ullmann, W.J., Aller, R.C., 1980. Dissolved iodine flux from estuarine sediments and implications for the enrichment of iodine at the sediment water interface. Geochim. Cosmochim. Acta 44, 1177–1184.

Waseda, A., Uchida, T., 2004. The geochemical context of gas hydrate. Resource Geol. 54, 69–78.